Highly Effective Antifungal and Antibacterial Properties of ZnO, ZnS, Fe$_2$S$_3$ and SnO Nanoparticles Against Various Fungal and Bacterial Isolates

Y. C. GOSWAMI*, RANJANA GOSWAMI and T. K. CHIROVA

Nano Lab, School of Sciences ITM University Gwalior Madhya Pradesh, 474001, India.
*Corresponding author E-mail: ycgoswami@gmail.com

ABSTRACT

This study explores the potential of four types of nanoparticles (ZnO, ZnS, FeS$_2$, and SnO$_2$) to combat resistant microbes using the well method. The research focuses on their antifungal and antibacterial properties. Results showed that FeS$_2$ and ZnO nanoparticles displayed broad-spectrum activity against various bacteria and fungi. This was evident by the formation of clear inhibition zones after 24 h at 37°C. These findings highlight the promise of FeS$_2$ and ZnO nanoparticles as weapons against resistant microbes. The inhibition zones demonstrate a measurable effect on microbial growth, providing valuable groundwork for further development of novel strategies to fight and manage microbial infections. This research adds to the ongoing search for alternative and effective solutions in the face of growing microbial resistance.

Keywords: Nanoparticles, Zinc sulphides, Antibacterial properties, Antimicrobial properties, Metal oxides, Metal sulphides, Zinc oxides.

INTRODUCTION

The emergence of antibiotic-resistant bacteria and fungi presents a significant challenge in healthcare. Widespread and often inappropriate use of antibiotics has fueled this resistance, rendering many existing treatments ineffective. This highlights the urgent need for novel antimicrobial solutions. Nanoparticles, particles typically between 1-100 nanometers in size, have emerged as a promising avenue in this fight. Their unique properties offer potential advantages over traditional antibiotics. Studies have shown nanoparticles to possess antimicrobial, anti-inflammatory, and wound-healing properties[6,7]. However, this field is still relatively young, and research on nanoparticle safety is ongoing.

A key concern with nanoparticles is their toxicity. Their small size, beneficial in many applications, can also increase their reactivity, potentially leading to harmful effects. Various factors influence toxicity, including size, surface area, and chemical composition[8,9]. These factors can interact, with combinations potentially leading to higher toxicity levels. Studies have shown a complex relationship between nanoparticle concentration and toxicity. In some cases, higher concentrations may lead to reduced toxicity due to particle aggregation,

hindering cellular uptake[10]. However, smaller nanoparticles, with easier cellular entry, may exhibit higher toxicity[11,12].

Despite these concerns, research suggests potential for safe and effective use of nanoparticles as antimicrobials. Green-synthesized ZnO nanoparticles have shown promise in combating bacterial and fungal pathogens[6]. However, other studies have highlighted the potential toxicity of nanoparticles towards non-targeted organisms[14].

This study focuses on evaluating the antifungal and antibacterial activity of four specific nanoparticles: ZnO, ZnS, FeS_2, and SnO_2. We aim to assess their effectiveness against various fungal and bacterial isolates. The study will also investigate the influence of concentration on their activity. By exploring these aspects, we hope to contribute valuable knowledge to the development of safe and effective nanoparticle-based antimicrobials.

MATERIALS AND METHODS

Materials
Fungal and Bacterial Isolates
Fungal isolates *(Aspergillus niger* and *Aspergillus fumigatus)* and bacterial isolates *(Escherichia coli, Bacillus cereus*, and *Bacillus subtilis)* were obtained from the Microbiology lab. These isolates were stored at 4°C and revived by culturing them on Sabouraud Dextrose Agar (SDA) or Nutrient Agar (NA) at 37°C for 24 hours.

Methods: Nanoparticle Synthesis
A modified hydrothermal method with dual precipitation and ultrasonication was used to synthesize SnO_2, ZnS, FeS_2, and ZnO nanoparticles. The synthesis involved following steps:

Step 1: Preparation of precursor solutions: Separate solutions of 0.1 M $ZnSO_4•7H_2O$ and 0.3 M Na2S were prepared in 10 mL DI water with stirring.

Step 2: SnO_2 synthesis: 0.1 M $SnCl_2•2H_2O$ was dissolved in a mixture of 20 mL DI water and 20 mL ethanol. After adding 0.1 M NH_4NO_3, the solution was stirred for 30 min at 50°C.

Antifungal activity assay
Sabouraud Dextrose Agar (SDA) media

was prepared (100 mL) and autoclaved (121°C, 15 psi for 15 minute). Six Petri dishes were also autoclaved. The sterilized media was poured into the Petri dishes and allowed to solidify within a Laminar Airflow Cabinet. Using a sterile 6 mm borer, two wells were created on opposite sides of the solidified media in four plates. Two of these plates were inoculated with *Aspergillus niger* and the other two with *Aspergillus fumigatus* using a spreader for even distribution. One plate served as the positive control (inoculated with fungi only) and another as the negative control (no fungi). The experiment evaluated the impact of synthesized nanoparticles on fungal growth.

Antibacterial activity assay
Nutrient Agar media (100 mL) was prepared and autoclaved along with six Petri dishes (121°C, 15 psi for 15 minute). The media was then poured and allowed to solidify in the plates. Similar to the antifungal assay, wells were created in four plates using a sterile 6 mm borer. Bacterial suspensions were prepared for *E. coli, Bacillus subtilis*, and *Bacillus cereus* by suspending bacteria in sterilized water. Each suspension was spread on separate plates using a sterile spreader. One plate served as the positive control (inoculated with bacteria) and another as the negative control (no bacteria). Varying concentrations (15 µL, 20 µL, 25 µL, and 30 µL) of each nanoparticle (ZnO, FeS_2, SnO_2, or ZnS) were loaded into one well per plate using a micropipette. An equal volume of ethanol was loaded into the opposite well as a control. The plates were incubated at 37°C for 24 h to allow bacterial growth. After incubation, the plates were examined for zones of inhibition around the wells containing nanoparticles or ethanol. The diameter of any inhibition zone was measured and recorded. The entire antibacterial activity assay was repeated three times for each bacteria-nanoparticle combination to ensure reliable results.

The modified hydrothermal method with dual precipitation and ultrasonication synthesised the SnO_2, ZnS, FeS, ZnO nanocomposite. The synthesis process involved three main steps. In the first step, separate 0.1M $ZnSO_47H_2O$ and 0.3M Na2S aqueous solutions were prepared in 10 mL DI water separately with continuous stirring. The presence of ZnS nanoparticles in the resulting milky white solution was confirmed using UV-Vis spectroscopy.

For SnO$_2$, 0.1M SnCl$_2$2H$_2$O was dissolved in a mixture of 20 mL DI water and 20 mL ethanol, followed by the addition of 0.1M NH$_4$NO$_3$. The solution was stirred for 30 minutes at 50°C, resulting in a milky white solution containing SnO$_2$ nanoparticles, which was confirmed using UV-Vis spectroscopy. Characterization of these nanoparticles was carried out with a reported concentration of 0.5M in 50cc of ethanol[19-22].

RESULTS AND DISCUSSION

Antifungal studies

The experiment evaluated the antifungal activity of synthesized nanoparticles (FeS$_2$, ZnO, SnO$_2$, and ZnS) against *Aspergillus niger*. Zone of inhibition formation and diameter were used to assess efficacy. Diameter of zone of inhibition results produced by nanoparticles at varying concentrations against *A. niger* shown in Figure 1.
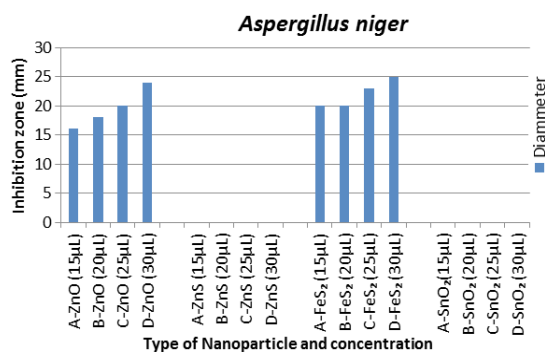

Fig. 1. Diameter of zone of inhibition results produced by nanoparticles at varying concentrations against *A. niger*

Figure 1 shows that FeS$_2$ and ZnO nanoparticles consistently produced inhibition zones against *A. niger* at all tested concentrations. In contrast, SnO$_2$ and ZnS did not exhibit any inhibitory effect at any concentration. The presence of inhibition zones indicates potential fungicidal activity, possibly linked to reactive oxygen species (ROS) production, which aligns with previous research[6].

The diameter of the inhibition zone increased with increasing concentrations of FeS$_2$ and ZnO, suggesting a dose-dependent antifungal effect. Both nanoparticles impeded fungal growth near the loaded wells. Interestingly, FeS$_2$ displayed stronger antifungal activity compared to ZnO. At the lowest concentration (15 μL), FeS$_2$ produced a 20 mm zone of inhibition compared to ZnO's 16 mm. This trend continued at higher concentrations (25 mm for FeS$_2$ vs. 24 mm for ZnO at 30 μL). Notably, FeS$_2$ exhibited

the same inhibition zone diameter (20 mm) at 15 μL and 20 μL concentrations, suggesting a possible plateau effect, where further concentration increase may not significantly enhance antifungal activity. This aligns with the concept of dose-dependent nanoparticle toxicity[25].

Our findings contradict observations by[23] who suggested that higher concentrations might not be effective due to aggregation. In contrast, this study demonstrates increased toxicity of FeS$_2$ and ZnO at higher concentrations. Conversely, SnO$_2$ and ZnS lacked any inhibitory effect, potentially indicating lower *A. niger* susceptibility or limited nanoparticle toxicity against this fungus. This difference in inhibition zones between ZnO and FeS$_2$ highlights the varying susceptibility of fungi to different nanoparticle types[25-27].

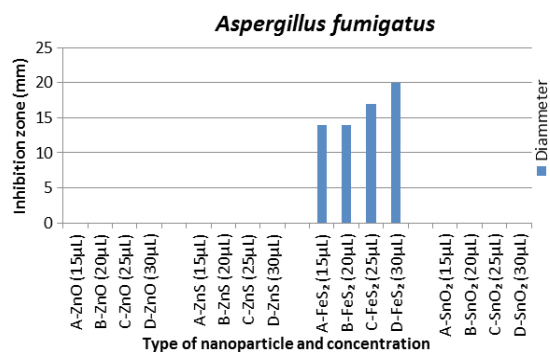As depicted in Fig. 2, the results highlight

Fig. 2. Diameter of zone of inhibition results produced by nanoparticles at varying concentrations against *A. fumigatus*

FeS$_2$ nanoparticles as the sole contributor to antifungal activity against *A. fumigatus*, evident in the production of zones of inhibition (as illustrated in Fig. 3). In contrast, ZnS, SnO$_2$, and ZnO nanoparticles yielded negative results, failing to produce distinct zones of inhibition. This absence of clear zones may suggest that *A. fumigatus*, as a fungal species, was less susceptible to the toxic effects exerted by the nanoparticles.

Examining Fig. 2 further, it is noted that FeS$_2$ at concentrations of 15 μL and 20 μL displayed identical zone of inhibition diameters of 14 mm, indicating that an increase from 15 μL to 20 μL did not enhance antifungal activity. This similarity mirrors the anomaly observed in the results against *A. niger*, suggesting that this concentration range may not significantly affect the activity against the fungi. However, FeS$_2$ exhibited smaller zones

of inhibition against *A. fumigatus* compared to *A. niger*, suggesting a potential variation in sensitivity or resistance between the two fungal strains.[17] emphasized that the toxic effects of nanoparticles on microorganisms depend not only on the nanoparticle type but also on the microbial species involved, which aligns with the observed differences in sensitivity.

FeS$_2$' antifungal efficacy against A. fumigatus (with a maximum zone of inhibition of 20 mm) was less pronounced than its impact on *A. niger* (with a minimum zone of inhibition of 20 mm). This disparity may indicate that *A. fumigatus* is a more resistant strain, producing smaller zones of inhibition. This inference is reinforced by the observation that ZnO, effective against *A. niger*, only managed to restrict the growth of *A. fumigatus* near the well, without clear zones of

inhibition. This discrepancy suggests the possibility that increasing the concentration of ZnO beyond 30 µL might be necessary for the production of distinct zones of inhibition.

It is noteworthy that the wells loaded with ethanol did not hinder fungal growth, signifying that all observed antifungal activity is solely attributed to the nanoparticles. In summary, with regard to antifungal activity, FeS$_2$ demonstrated superior efficacy, followed by ZnO nanoparticles. The mechanism of action involves the disruption of the cell membrane, leading to cellular disruption and death, coupled with the production of radical oxygen species that are detrimental to cell organelles[6],[22-23]. Furthermore, the maintenance of inhibition zones after 48 h indicates the sustained effectiveness of nanoparticles in their fungicidal activity, also reflecting proper diffusion within the agar media.
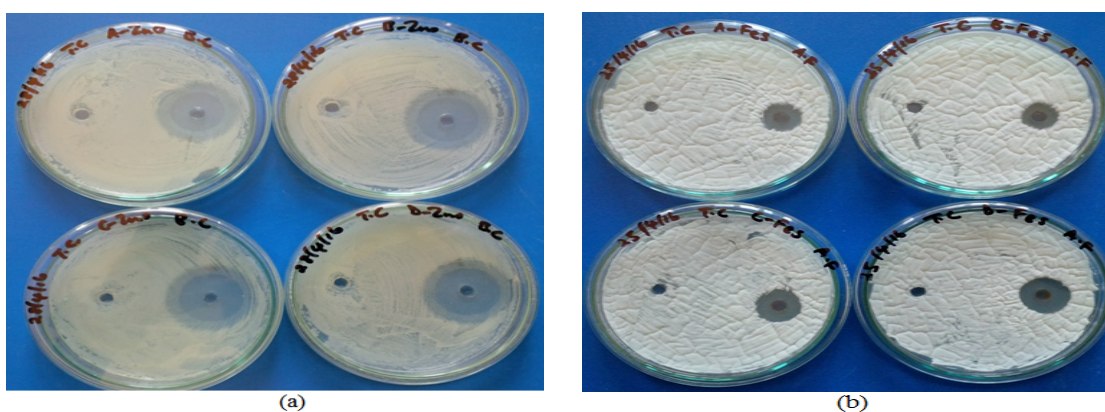

(a)   (b)

Fig. 3. Images showing the zone of inhibition exerted by (A) ZnO nanoparticles against *Bacillus cereus* and (B) FeS$_2$ nanoparticles against *Aspergillus fumigatus*

Antibacterial studies

Figure 3 demonstrates the formation of clear inhibition zones around wells containing ZnO and FeS$_2$ nanoparticles against *Bacillus cereus*. This observation suggests the nanoparticles' ability to diffuse through the media and inhibit bacterial growth, potentially indicating bactericidal activity[6]. The presence of inhibition zones aligns with previous research highlighting the nanoparticle's potential to impede bacterial growth.

Figure 4 shows the concentration-dependent antibacterial activity of ZnO, FeS$_2$, SnO$_2$, and ZnS against *Bacillus cereus*. ZnO consistently produced the largest inhibition zones at all tested concentrations, followed by SnO$_2$, FeS$_2$, and ZnS. Notably, ZnO exhibited a larger zone (25 mm) at 20 µL compared to the highest concentration of

ZnS (17 mm), SnO$_2$ (24 mm), and FeS$_2$ (23 mm). ZnO reached its maximum zone size (26 mm) at 30 µL, while ZnS had the smallest zone (17 mm) at the same concentration.
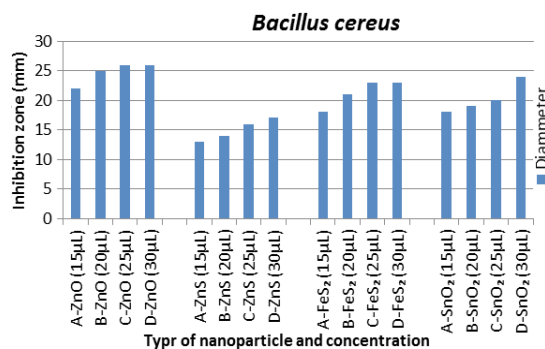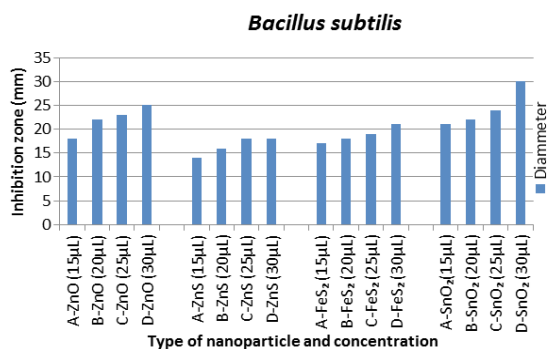

Fig. 4. Diameter of zone of inhibition results produced by nanoparticles at varying concentrations against *Bacillus cereus*

Interestingly, all nanoparticles except ZnO and FeS$_2$ displayed increasing inhibition zones with higher concentrations. This aligns with the concept of concentration-dependent nanoparticle toxicity[6,17, 30].

The observed variations in bacterial growth inhibition support previous findings[17] that nanoparticle toxicity depends on both nanoparticle type and bacterial species. After 48 h, clear inhibition zones remained for ZnO, ZnS, and FeS$_2$, while SnO$_2$ showed bacterial growth within the zone. This could be due to a decrease in SnO$_2$ nanoparticle concentration as bacterial cells divided, reducing the observed antibacterial effect[31,32].

Furthermore, *Bacillus cereus* demonstrated higher susceptibility to ZnO and lower susceptibility to ZnS, highlighting species-specific sensitivity to nanoparticles, as reported by[17].

Fig. 5. Diameter of zone of inhibition results produced by nanoparticles at varying concentrations against *Bacillus subtillis*

Figure 5 demonstrates the concentration-dependent antibacterial activity of ZnO, FeS$_2$, SnO$_2$, and ZnS against *Bacillus subtilis*. SnO$_2$ displayed the largest inhibition zones for all concentrations except 20 µL, where it matched ZnO and FeS$_2$ and showed moderate effectiveness, while ZnS had the weakest effect. Notably, SnO$_2$ consistently exhibited larger inhibition zones compared to other nanoparticles.

Maximum inhibition for SnO$_2$ was observed at 30 µL (30 mm zone), while ZnS had the smallest zone (18 mm) at the same concentration. All nanoparticles displayed increasing inhibition zones with higher concentrations, aligning with the concept of concentration-dependent nanoparticle toxicity[6, 17,31].

Similar to *B. cereus*, these findings suggest bacterial species and nanoparticle type influence

toxicity[17]. *B. subtilis* showed varying sensitivity, with SnO$_2$ being the most effective, followed by ZnO, FeS$_2$, and ZnS.

After 48 h, clear inhibition zones remained for ZnO, ZnS, and FeS$_2$, while SnO$_2$ showed bacterial growth within the zone. This might be due to a decrease in SnO$_2$ nanoparticle concentration as bacteria divided, reducing the observed effect[32,33].

In conclusion, SnO$_2$ exhibited the strongest antibacterial activity against *B. subtilis*, followed by ZnO, FeS$_2$, and ZnS. This study highlights the importance of considering both nanoparticle type and bacterial species for effective antibacterial applications.
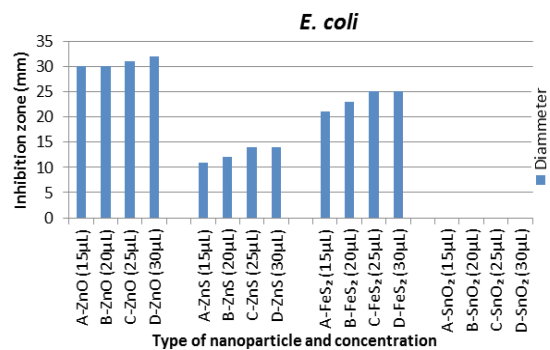
Fig. 6. Diameter of zone of inhibition results produced by nanoparticles at varying concentrations against *E. coli*

Figure 6 presents the outcomes of the assessment of test nanoparticles against *E. coli*. Results indicated that all nanoparticles, with the exception of SnO$_2$, were able to generate inhibition zones against *E. coli*. The most notable inhibition zone was observed for ZnO nanoparticles at 30 µL, displaying a 32 mm inhibition zone. Following ZnO, FeS$_2$ exhibited a 25 mm inhibition zone, and ZnS showed a 14 mm inhibition zone at the same concentration for those nanoparticles that produced an inhibition zone. ZnO emerged as the most effective against *E. coli*, consistently producing the largest inhibition zones for all concentrations compared to the other test nanoparticles.

Consistent with prior research[6,17] and supported by[30], which emphasizes the concentration-dependent nature of nanoparticle toxicity, the results for *E. coli* in this study aligned with the notion that inhibition zones tend to increase with higher concentrations. This pattern was observed for all test nanoparticles except SnO$_2$, which did not

produce any inhibition zone for all concentrations. This finding is in line with[17], indicating that each species possesses a specific susceptibility to certain nanoparticles, and in the case of *E. coli*, it demonstrated insensitivity or resistance to SnO_2 nanoparticles.

The results highlighted the heightened sensitivity of *E. coli* to ZnO nanoparticles, and all test nanoparticles maintained clear inhibition zones even after 48 h of culture. This persistence underscores the sustained antibacterial effectiveness of the nanoparticles against *E. coli*.

Key findings
Antibacterial activity

ZnO nanoparticles exhibited the strongest and most consistent antibacterial effect across all bacterial isolates *(Bacillus cereus, Bacillus subtilis,* and *E. coli)*. This is likely due to ZnO's ability to disrupt bacterial cell membranes, leading to cell death. Their small size facilitates membrane penetration, causing stress and breakdown. FeS_2 nanoparticles also displayed consistent antibacterial activity against all isolates, potentially through the generation of reactive oxygen species that damage bacterial cells. ZnS nanoparticles showed moderate and consistent antibacterial activity, while SnO_2 was only effective against *Bacillus species*. This highlights the dependence of nanoparticle toxicity on both nanoparticle type and bacterial species. Bacillus cereus was the most susceptible bacteria, followed by *Bacillus subtilis* and then *E. coli*. This aligns with previous research suggesting *E. coli's* lower susceptibility to nanoparticles compared to *Bacillus subtilis*.

Antifungal activity

FeS_2 nanoparticles were the most effective against the fungal isolate *(Aspergillus niger)*, followed by ZnO nanoparticles. Both inhibited fungal growth by creating clear inhibition zones. Their mechanism of action likely involves disrupting fungal cell membranes and producing cell-damaging radical oxygen species. Importantly, the inhibition zones remained after 48 h, indicating sustained fungicidal activity SnO_2 and ZnS did not exhibit any antifungal activity against *A. niger*. This study supports the concept that nanoparticle effectiveness depends on both the type of nanoparticle and the specific microorganism (bacteria or fungi) being targeted Bacteria displayed greater overall susceptibility to the tested nanoparticles compared to fungi.

CONCLUSION

This study investigated the antibacterial and antifungal activity of synthesized ZnO, FeS_2, SnO_2, and ZnS nanoparticles. ZnO nanoparticles demonstrated the strongest and most consistent antibacterial effect against various bacteria *(Bacillus cereus*, *Bacillus subtilis*, and *E. coli)*. FeS_2 nanoparticles also displayed broad-spectrum antibacterial activity. Fungal susceptibility was lower compared to bacteria. FeS_2 nanoparticles exhibited the most effective antifungal activity against *Aspergillus niger*, followed by ZnO nanoparticles. SnO_2 and ZnS lacked antifungal properties against this fungus. Both bacterial and fungal susceptibility varied depending on the nanoparticle type, highlighting the importance of considering this factor in developing nanoparticle-based antimicrobial applications. This study provides valuable insights into the potential of these nanoparticles for developing targeted antimicrobial agents. Further research is necessary to ensure their safe and effective application.

Conflict of interest
The author declare that we have no conflict of interest.

REFERENCES

1. Vaseem, M.; Umar, A.; Yoon-Bong, H., *Am. Sci. Pub.*, **2010**, *5*, 1-36.
2. Bisauriya, R.; Verma, D.; Goswami, Y.C., *J. Mater. Sci: Mater Electron.*, **2018**, *29*, 1868–1876.
3. Kumar, N.; Purohit, L.P.; Goswami, Y.C., *AIP Conf. Proc.*, **2015**, *1675*, 020030.
4. Liu, W., *J. Biosci. Bioeng.*, **2006**, *102*, 11-7.
5. Sungkaworn, T.; Triampo, W.; Nalakarn, P.; Triampo, D.; Tang, I.M.; Lenbury Y., *Int. J. Biomed. Sci.*, **2007**, *2*, 67-74.
6. Kumar, N.; Purohit, L.P.; Goswami, Y.C., *Chal. Lett.*, **2015**, *12*, 333-338.

7. Kumar, N.; Pathak, T.K.; Purohit L.P.; Swart, H.C.; Goswami, Y.C., *Nano-Struct. Nano-Objects.,* **2018**, *16*, 1-8.

8. Hajipour M.; Fromm K.; Ashkarran, A.K.; Aberasturi, D. J.; Larramendi, I.; Rojo, T.; Serpooshan, V.; Parak, W.; Mahmoudi, M., *Trends in Biotech.,* **2012**, *30*, 499-511.

9. Vandeputte, P.; Ferrari S.; Coste, A., *Int. J. Microbio.,* **2012**, *2012*, 1-26.

10. Gunalan, S.; Sivaraj R.; Rajendran, V., *Progress in Nat. Science: Mater. Internat.,* **2012**, *22*, 693-700.

11. Taylor, P.L.; Ussher, A.L.; Burrell, R.E., *Biomaterials.,* **2005**, *26*, 7221-7729.

12. Merlin, J. P.; Xiaogang L., *Front. Gen.,* **2022**, 12, 10.3389/fgene.2021.817974.

12. Buzea, A.; Pacheco, I.; Robbie, K., *Biointer-phases.,* **2007**, *2*, MR17.

13. Gurr, J.; Wang, A.; Chen, C.; Jan; K., *Toxicol.,* **2005**, *213*, 66-73.

14. Kumar, V.; Rajaram, P.; Goswami, Y.C., *J. Mat. Sci.: Mat. Elect.,* **2017,** *28*, 9024-9031.

15. Goswami, Y.C.; Mohapatra, R.; Kaundal, J. B., *Chalcogenide letters.,* **2021**, *18*, 255-262.

16. Sharma, R.; Singh, R.; Goswami, Y.C.; Kumar V.; Kumar, D., *J. Aust. Ceram. Soc.,* **2021**, *57*, 697-703.

17. Kumar, N.; Purohit, L. P.; Goswami, Y.C., *Physica E: Low-dim. Sys. Nano.,* **2017**, *83*, 333-338.

18. Goswami, Y.C.; Kumar, V.; Rajaram, P., *Mat. Lett.,* **2014**, *128*, 425-428.

19. Lakshminarayanan, V.; Bhattacharya, I., *Advances in Optical Science and Engineering, Springer Proceedings in Physics.,* **2014**, *166*, 533-539.

20. Nagaich, S.; Goswami, Y.C., *Fifth International Conference on Advanced Computing & Communication.,* **2015**, *5*, 165-168 doi: 10.1109/ACCT.2015.16

21. N Kumar.; N LP Purohit.; L.P. YC Goswami.; Y. C., *Physica E: Low-dim. Sys. Nano.,* **2016**, *83*, 333-338.

22. Singh, R.; Kumar, D.; Goswami, Y.C.; Sharma; R., *Arab. J. Chem.,* **2019**, *12*, 1537-1544.

23. Kumar, N.; Purohit, L.P.; Goswami Y. C., *AIP Conf. Proc.,* **2015**, *1675*, 020030.

24. Sharma, R.; Singh, B.; Kumar, V.; Goswami, Y. C.; Singh, R.; Kumar, D., *Adv. Opt. Sci. Eng.,* **2015,** 575-580.

25. Takenaka, S.; Karg, E.; Roth, C.; Schulz, H.; Ziesenis, A.; Heinzmann, U.; Schramel P.; Heyder., *J. Env. Health Persp.,* **2001**, *109*, 547.

26. Oberdörster, G.; Oberdörster, E.; Oberdörster., *J. Env. Health Persp.,* **2005,** *113*, 823-839.

27. Jones, N.; Ray, B.; Ranjit, B.K.; Manna, A., *FEMS Microbio. Lett.,* **2008**, *279*, 71-76.

28. Aruoja, V.; H. Dubourguier, H.; Kasemets K.; Kahru, A., *Sci. Total Env.,* **2009**, *407*, 1461-1468.

29. Baek Y.; An, Y.; *Sci. Total Env.,* **2011,** *409*, 1603-1608.

30. Brayner, R.; Ferrari-Iliou, R.; Brivois, R.N.; Djediat, S. Benedetti M. Fiévet, F., *Nano Lett.,* **2006**, *6*, 866-870.

31. Padmavathy N.; Vijayaraghavan, R., *Sci. Tech. Adv. Mat.,* **2008**, 9035004.

32. Huang, Z.; Zheng, X.; Yan, D.; Yin, G.; Liao, X.; Kang, Y.; Yao, Y.; Huang, D.; Hao, B., *Langmuir.,* **2008**, *24*, 4140-4144.